Solid State Communications 254 (2017) 15–20

Contents lists available at ScienceDirect

Solid State Communications

journal homepage: www.elsevier.com/locate/ssc

Communication

The electronic properties of concentric double quantum ring and possibility designing XOR gate

Lafy. F. AL-Badry

Department of Physics, Faculty of Science, Thi Qar University, Nassiriya 64000, Iraq

ARTICLE INFO

Communicated by R. Merlin

Keywords:
A. Concentric double quantum ring
C. XOR gate
D. Aharonov–Bohm effect
D. Conductance
D. I-V characteristics

ABSTRACT

In this paper I have investigated the Aharonov–Bohm oscillation in concentric double quantum ring. The outer ring attached to leads while the inner ring only tunnel-coupled to the outer ring. The effect of inner ring on electron transport properties through outer ring studied and found that the conductance spectrum consists of two types of oscillations. One is the normal Aharonov–Bohm oscillation, and other is a small oscillations superposed above AB oscillation. The AB oscillation utilized to designing nanoscale XOR gate by choosing the magnetic flux and tuning the gate voltages which realization XOR gate action.

1. Introduction

Quantum rings have proven to be an interesting field of study because of their geometry structure and their potentiality as a base of quantum information technologies and for novel optoelectronic devices [1–6]. Quantum rings are nanoscale conductor or semiconductor rings have few electrons. Furthermore, quantum ring structures distinguishing from quantum dots by exhibiting the Aharonov-Bohm (AB) effect [7]. This has permitted to study the Aharonov-Bohm effect of the nanostructures, which can be clearly observed in the electron transport spectrum at a magnetic field is perpendicularly applied to quantum rings [8]. Therefore, an oscillation of magnetization and periodic dependence of conductance spectrum in quantum rings are the simplest appearance of the AB effect. The first investigation into Aharonov-Bohm effect of normal metal rings was studied by Webb et al. [8].

In a concentric configuration, an inner ring is insulated and centered inside an outer ring [9]. The concentric configuration of quantum rings reveals significant features. The transition between the outer and the inner ring is analogous to atomic phenomena [10]. The inter-ring tunnel coupling and the geometry factors of rings such as size and shape become important [11]. In the past decade, a number of papers were devoted to the experimental and theoretical investigation, which are grounded on the influence of magnetic and electric fields on the electronic and visual properties of concentric double quantum rings. Climente et al. theoretically calculated electronic structures of the concentric quantum double rings [12]. For instance, Escartín et al. theoretically investigated influence the perpendicularly applied magnetic field on few-electron states in the concentric double quantum ring using local spin-density functional theory [13]. In addition, in Ref. [14] one-electron states and intraband absorption of concentric double quantum rings dependence on a lateral electric field are investigated. The influence of hydrostatic pressure and magnetic field on an artificial hydrogen molecule confined in a double concentric quantum ring is considered [15]. This study showed that the external magnetic field tuning the artificial hydrogen molecule energy structure. The effects of donor impurity on the energy spectrum and energy gaps in concentric triple quantum nanoring were studied by Salehani et al. [16]. Mühle et al. were experimentally studied electronic transport across the outer ring of a concentric double quantum ring attachment to electrodes under a magnetic field was perpendicularly applied in two works [9,17].

Most of the theoretical works about concentric quantum rings found in the literature do not discuss open systems since the focus lies on close systems. This motivated us to study electron transport properties through the concentric double quantum ring as an open system. In other words, the electrodes attached to the concentric double quantum ring. To the best of our knowledge, the influence of magnetic flux on electron transport through the concentric double quantum ring (CDQR) structures as an open system have not been theoretically investigated. In present work, the concentric double quantum ring structure is considered for studying electron transport properties and utilizing this structure to design XOR gate based on AB effect. The structure consists of an outer ring connected to the donor and acceptor, where the donor attached to left lead and the acceptor attached to the right lead. The inner ring is electrically isolated from the outer ring. Two gate voltages are externally applied to outer ring for controlling the energies of their atomic sites.

Several promising applications for this field, such as quantum logical elements and quantum bits [18–20]. The quantum logic circuits can be created by arranging the quantum rings in series [21–23]. The paper is structured as follows. The theoretical model presented in Section 2, the results and discussions are dedicated to Section 3, and Section 4 contains the conclusion.

http://dx.doi.org/10.1016/j.ssc.2017.02.007
Received 14 November 2016; Received in revised form 9 February 2017; Accepted 15 February 2017
Available online 17 February 2017

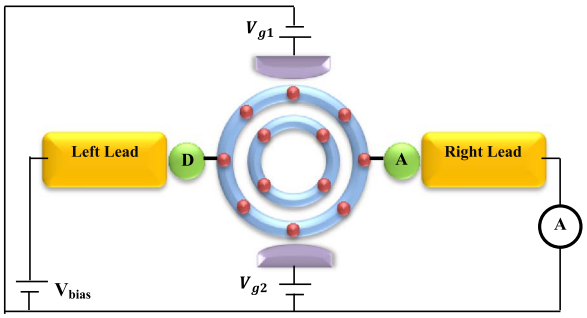

Fig. 1. (Color online) The scheme of concentric double quantum ring attached to donor and left lead from left side, and attached to acceptor and right lead from right side.

2. Theoretical model

The considered system is presented in Fig. 1, where a concentric double quantum ring CDQR is sandwiched between a donor and an acceptor, the donor (the acceptor) is connected to the left lead (right lead). CDQR is composed of two normal metallic rings, an inner ring consists of four atomic sites, while the outer ring consists of eight atomic sites. CDQR is threaded by a magnetic flux Φ, the so-called Aharonov-Bohm (AB) flux. The strength of site energies in the atomic sites of outer ring can be tuned by applying the two external gate voltages. The gate voltages V_{g1} and V_{g2} are externally applied to upper and lower arm of the outer ring, respectively. These gate voltages are variable and represent two inputs of the XOR gate. These two gate electrodes are isolated from the outer ring.

The Hamiltonian which describes this system can be written as,

$$H(t)=H_E(t)+H_{DBA}(t)+H_{LR}(t), \tag{1}$$

where,

$$H_E(t)=\sum_{\sigma,\alpha=D,A} E_\alpha n_{\sigma,\alpha}(t)+\sum_{m=1,\sigma}^{4} E_{m\sigma} n_{m\sigma}(t)+\sum_{n=1,\sigma}^{8} E_{n\sigma} n_{n\sigma}(t)+V_{g1} \sum_{\sigma} C^{\dagger}_{3\sigma}(t)C_{3\sigma}(t)+V_{g2}\sum_{\sigma} C^{\dagger}_{7\sigma}(t)C_{7\sigma}(t)+\sum_{\sigma,\beta=L,R} E_{k\beta} n_{\sigma k\beta}(t)+\sum_{i} U_i n_{i\uparrow} n_{i\downarrow}, \tag{2}$$

it describes energy levels of donor ($\alpha = D$), acceptor ($\alpha = A$), atomic sites of the inner ring ($m = 1,\ldots,4$), atomic sites of the outer ring ($n = 1,\ldots,8$), left lead ($\beta = L$), and right lead ($\beta = R$). V_{g1} and V_{g2} represent gate voltages externally applied on the outer ring. The strength of on-site Coulomb interaction is U_i. The index k_β represents wave vector of electron in the lead β. The occupation number is $n_{j\sigma}(t) = C^{\dagger}_{j\sigma}(t)C_{j\sigma}(t)$ and the $C^{\dagger}_{j\sigma}(t)(C_{j\sigma}(t))$ announces the creation (annihilation) operators of electron in subsystem j with spin $\sigma(=\uparrow,\downarrow)$. $H_{DBA}(t)$ represents the coupling interaction between the donor with the first atomic site of the outer ring V_{D1}, the coupling interaction between the acceptor with the fifth atomic site of the outer ring $V_{A,5}$, the nearest-neighbor hopping integral between the atomic sites in every ring V, and inter-ring tunnel coupling t.

$$H_{DBA}(t)=V_{D,1}\sum_{\sigma} C^{\dagger}_{D\sigma}(t)C_{1\sigma}(t)+V_{A,5}\sum_{\sigma} C^{\dagger}_{A\sigma}(t)C_{5\sigma}(t)+V\sum_{ij,\sigma}(e^{i\phi_{ou}}+e^{i\phi_{in}})C^{\dagger}_{i\sigma}(t)C_{j\sigma}(t)+t\sum_{ij,\sigma} C^{\dagger}_{i\sigma}(t)C_{j\sigma}(t)+H.\,C., \tag{3}$$

where Aharonov-Bohm phase factor of outer and inner ring are $\phi_{ou}=\pi\Phi/4\Phi_\circ$ and $\phi_{in}=\pi\Phi/2\Phi_\circ$ respectively, Φ is the magnetic flux, and $\Phi_\circ=ch/e$ is the flux quantum. $H_{LR}(t)$ describes the tunneling between donor and left lead from the left side V_{Dk_L}, and the tunneling between the acceptor and the right lead from the other side V_{Ak_R},

$$H_{LR}(t)=\sum_{\sigma,k_L} V_{D,k_L} C^{\dagger}_{D\sigma}(t)C_{k_L\sigma}(t)+\sum_{k_R} V_{A,k_R} C^{\dagger}_{A\sigma}(t)C_{k_R\sigma}(t)+H.\,C. \tag{4}$$

The first-order derivative for the equations of motion can be obtained by using formula,

$$\dot{C}_{j\sigma}(t)=-i\frac{dH(t)}{dC^{\dagger}_{j\sigma}(t)}. \tag{5}$$

The system approaches a steady state at long time, where the amplitude of each state oscillates corresponding to $C_{j\sigma}(t)=\overline{C}_{j\sigma}(E)e^{-iEt}$. The equations resulted from the above mathematical treatment can be written as a matrix. By using the same steps in the reference [24], transmission probability amplitude was obtained by using the relation $t(E)=\overline{C}_A/\overline{C}_D$ as,

$$t(E)=\frac{\frac{V_{A,5}\Delta_{5D}}{\Delta}}{E-E_A-\frac{V_{A,5}\Delta_{5A}}{\Delta}-\sum_{AR}(E)}, \tag{6}$$

where Δ,Δ_{5D} and Δ_{5A} are determinants occurring by matrix equation, while $\sum_{AR}(E)$is the self-energy of right lead. Consequently, the transmission probability of an electron through CDQR is given by,

$$T(E)=|t(E)|^2 \tag{7}$$

The transmission probability calculated by using Eq. (7) can be employed to determining the current–voltage (*I-V*) characteristics by the relation [25],

$$I=\frac{2e}{h}\int T(E)(f_L(E)-f_R(E))dE. \tag{8}$$

where $f_\beta(E)=1/(1+exp\frac{(E-\mu_\beta)}{k_BT})$ which represents Fermi distribution function of left and right leads, $\mu_L=E_F+eV/2$ and $\mu_R=E_F-eV/2$ are the chemical potentials for both leads, E_F is the equilibrium Fermi energy, k_B is Boltzmann constant, V is bias voltage, and T is the system temperature.

3. Results and discussions

All coupling strengths between subsystems were considered as $\gamma\Gamma$, where γ is a dimensionless parameter that represent the coupling strength in terms of Γ (where Γ is constant). Conveniently, all energy quantities were related to the coupling strength, and to have same energy units. Therefore, all energies and coupling strengths between subsystems were measured by units Γ.

Different parameters used for the calculations are described below. In CDQR, The outer ring-donor and outer ring-acceptor coupling strengths $V_{1,D}=V_{5,A}=\gamma\Gamma$ were considered, where $\gamma = 0.3$. The energies of the atomic sites were $E_m=0\Gamma$, the energy levels of donor and acceptor were $E_D=E_A=0\Gamma$. The Fermi energy at equilibrium was $E_F=0\Gamma$. The nearest-neighbor hopping strengths for both outer and inner ring were $V = 0.5\Gamma$. Inter-ring tunnel coupling is $t = 0.1\Gamma$, which allow to tunneling between two rings [26]. The gate voltage is one of the most significant factors which controls the electronic transmission of quantum rings. The electron transport properties are also highly sensitive to magnetic flux. To reveal these facts, the behavior of transmission spectrum was first analyzed and transmission probability was employed for calculating electrical properties.

3.1. Transmission probability characteristics

To control the effect of magnetic flux on transmission probability more transparently, the results in a logarithmic scale are presented in Fig. 2 for various values of magnetic flux. The transmission probability demonstrated sharp resonant peaks of most the energy eigenvalues. These resonant peaks are associated with eigenvalues of CDQR. The resonant peaks localization about energies $E = -0.7, 0,$ and 0.7Γ degenerate by increasing magnetic flux as shown in Fig. 2(a-d). Furthermore, antiresonances appear in transmission spectrum, some antiresonances are quite similar to a Fano-like behavior. These antiresonances are exhibited due to quantum interference between electron waves passing

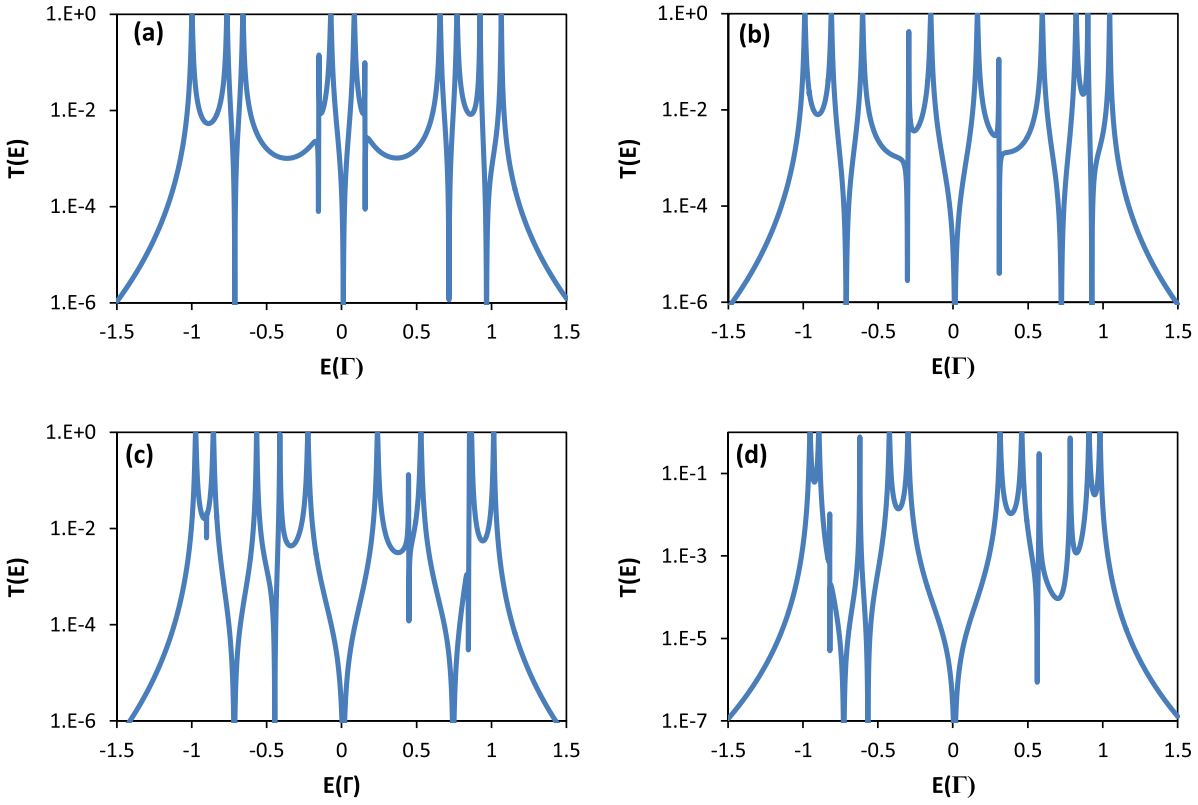

Fig. 2. Transmission as a function electron energy, (a) at $\phi = 0.2$, (b) at $\phi = 0.4$, (c) at $\phi = 0.6$, (d) at $\phi = 0.8$. Inter-ring tunnel coupling at $t = 0.1\Gamma$, without Coulomb interaction U=0.

through CDQR, the positions of antiresonances independent of magnetic flux. In an open system, quantum interference can be represented in terms of the interference pattern of de Broglie waves due to electrons passing through outer ring from left lead to right lead. The CDQR structure constitute a significantly good test case as the transmission probability through a structure controlled by destructive interference will be in completely contrast to one with constructive interference. The antiresonances appear because destructive interference, while constructive interference causes resonant peaks [27]. In Fig. 2(d), some the antiresonances die out because of the influence of magnetic flux.

The transmission probability as a function of electron energy passing through CDQR with different values of inter-ring coupling $t = 0.05,0.1 and 0.15\Gamma$ at $\phi = 2\pi$ is presented in Fig. 3. It is clearly observed that a significant change in the transmission spectrum gets at $\phi = 2\pi$, where the transmission probability reveals sharp resonant peaks of some specific energies. While it suppressed for all other energy values. All antiresonances suppressed by effect magnetic flux except that located at $E = 1\Gamma$. The situation becomes much interesting when the effect of inter-ring coupling is studied. It shows that the transmission spectrum of each value of inter-ring coupling has similar behavior,

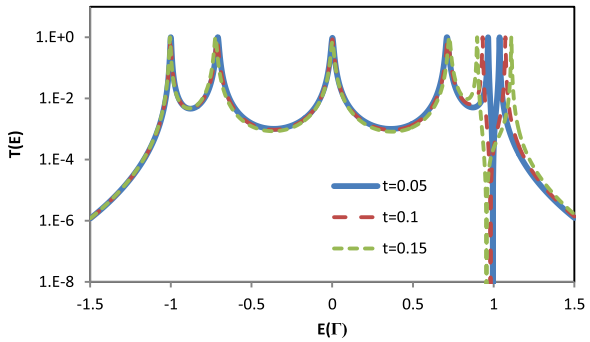

Fig. 3. The transmission probability as a function of energy with different values of inter-ring coupling $t = 0.05,0.1 and 0.15$, without Coulomb interaction U=0.

but the two resonances located about $E = 1\Gamma$ have not identical behavior. One observed that these two resonances become more degeneracy by increasing inter-ring coupling. Consequently, the inner ring obviously affect the transport properties.

3.2. Electrical conductance

The electrical conductance is calculated as a function of the magnetic flux at different values of gate voltages as shown in Fig. 4. Symmetric values of gate voltages are applied to the upper and lower arm of outer ring V_{g1}=V_{g2}=0.45,0.4,0.35,0.3V, which have been taken within the range of experimental values [17], as presented in Fig. 4(a). The peak of electrical conductance located at $\phi = n\pi$ where n is even. In contrast, the electrical conductance vanishes at $\phi = n\pi$ where n is odd. This behavior can be attributed to the normal Aharonov-Bohm effect of electrons passing through the outer ring [17]. The AB oscillate gives a surprising behavior in designing nanoscale XOR gate by choosing the magnetic flux that creates peak or dip of conductance spectrum. While, the small oscillations appear above AB oscillations because of the influence of tunnel coupling between the outer ring and inner ring. In Ref. [28,29], Kusmartsev shows fractional oscillations in quantum rings are related to ratio the Coulomb into the hoping parameters and depending on ratio the number of electrons into the number of sites in quantum ring.

The oscillations amplitude decreases whenever gate voltage increases. The behavior of the small oscillations depending on the values of gate voltages symmetrically applied to the outer ring. The electrical conductance has a maximum value (0.44) at V_g=0.3V. The electrical conductance is calculated as a function of magnetic flux at asymmetric values of the gate voltages V_{g1}=0.45,0.4,0.35,and0.3V with a fixed value of lower gate voltage V_{g2}=0, as clearly highlighted in Fig. 4(b). As a result, the electrical conductance is monotonically increasing when the gate voltage is reduced, it is access to 0.95 at V_{g1}=0.3V. The small oscillations have the same behavior for all gate voltages, therefore it independent of the asymmetric values of gate voltages. The same result proved by

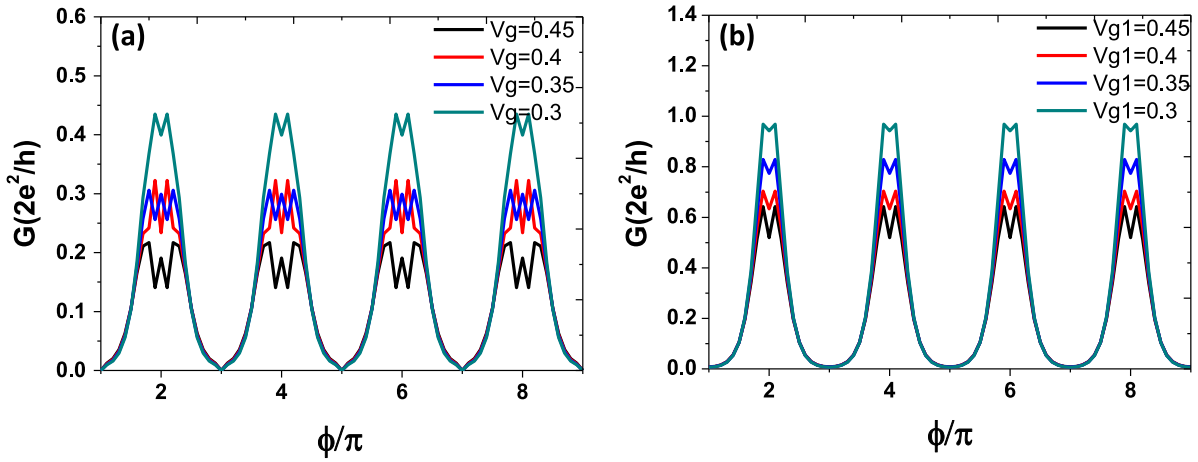

Fig. 4. Electrical conductance as a function of the magnetic flux at inter-ring coupling $t = 0.1$, without Coulomb interaction U=0, with several values of gate voltages (a) V_{g1}=V_{g2}=0.45,0.4,0.35,and0.3V (b) V_{g2}=0 and V_{g1}=0.45,0.4,0.35,and0.3V.

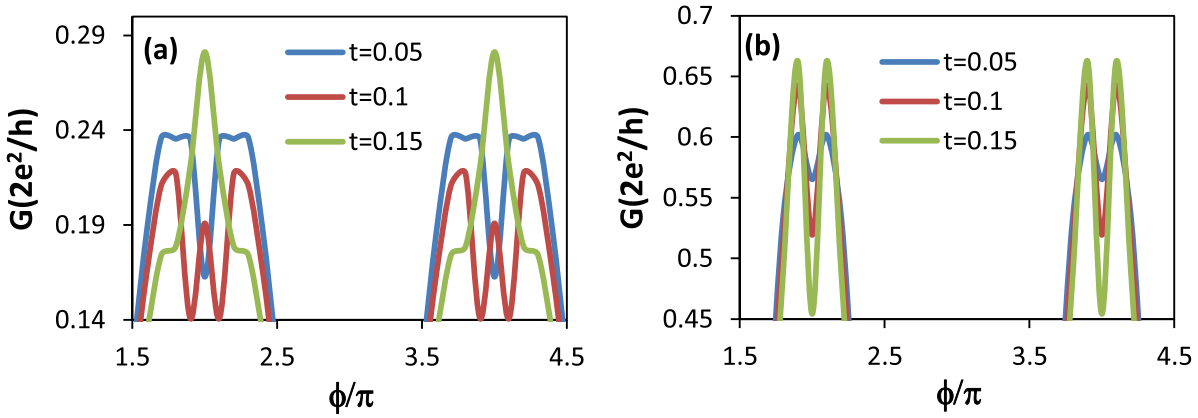

Fig. 5. Electrical conductance as a function of the magnetic flux at different values of inter-ring coupling t = 0.05,0.1,and0.15Γ without Coulomb interaction U=0, with gate voltage (a) V_{g1}=V_{g2}=0.45V. (b) V_{g1}=0.45 and V_{g2}=0.

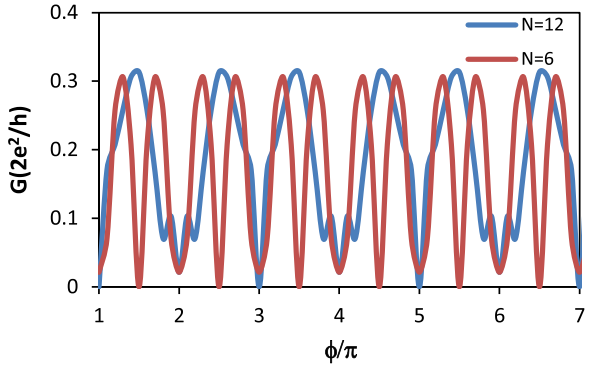

Fig. 6. Electrical conductance as a function of the magnetic flux at the number of electrons N=6, 12 and fixed value of the number of sites (12) with gate voltage Vg_1=Vg_2=0.45. Coulomb interaction U=1Γ.

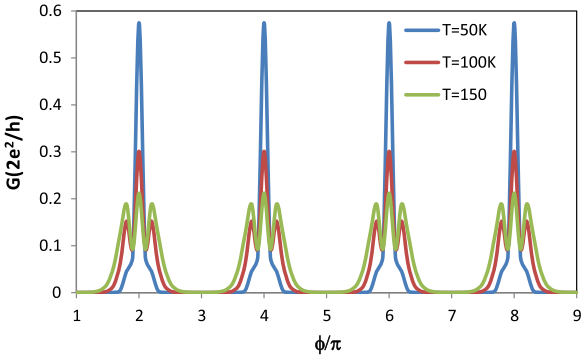

Fig. 7. Electrical conductance as a function of magnetic flux at different temperatures T=50,100, and 150 K.

Mühle et al. for symmetric values of gate voltages [17].

To enhance the clarity of the small oscillations are plotted as a function of the magnetic flux with different values of inter-ring tunnel coupling as presented in Fig. 5. In case both gate voltages are symmetric V_{g1}=V_{g2}=0.45V, that the small oscillations behave non-monotonic for the values of inter-ring tunnel coupling from 0.05 to 0.15Γ, as shown in Fig. 5(a). While in Fig. 5(b), these oscillations uniformly depend on values of inter-ring coupling in case upper and lower gate voltages are asymmetric.

In additionally, to understand the effect Coulomb interaction and the number of electrons on fractional oscillations, the electrical conductance is plotted as a function to the magnetic flux at U=1 for the number of electrons N=6, 12, as shown in Fig. 6. The electrical conductance increases with respect to Coulomb interaction. The periodicity of A-B oscillation decreases into half at N=6. In this case, the conductance spectrum vanishes at half integer of magnetic flux. The reason behind that behavior is the fractional oscillations of A-B period depend on ratio the number of electrons (N=6) to the number of sites (L=12).

The temperature dependent electrical conductance analyzed in Fig. 7. The Aharonov-Bohm oscillations in conductance spectrum are measured at three different temperatures T=50, 100, and 150 K. The small oscillations in electrical conductance are suppressed at the lowest

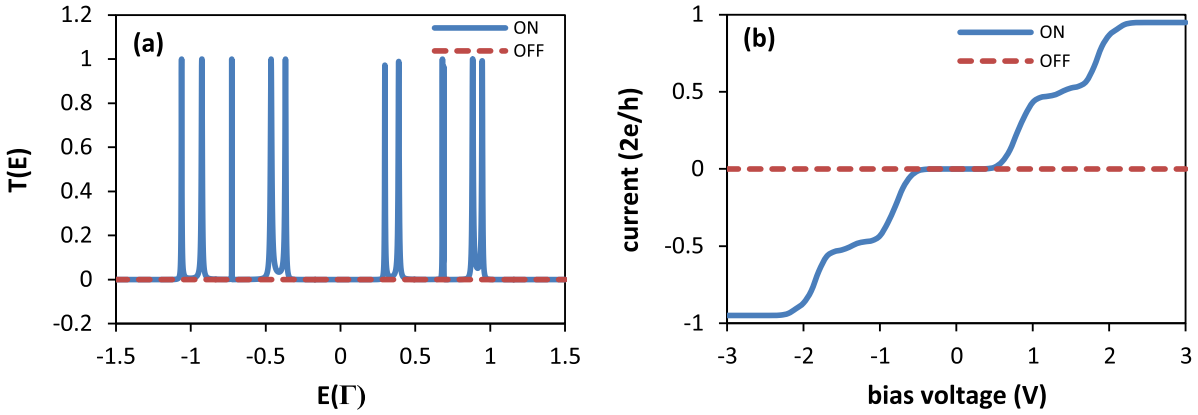

Fig. 8. (a): Transmission probability as a function of electron energy and (b): Electric current as a function of bias voltage. ON indicate to V_{g1}=0.4 and V_{g2}=0, or V_{g1}=0 and V_{g2}=0.4. OFF indicates to V_{g1}=V_{g2}=0, or V_{g1}=V_{g2}=0.4, where magnetic flux is Φ=Φ◦/2.

temperature. In contrast, the most important observation is the large reduction in conductance spectrum at higher temperature T=150. As a result, inter-ring coupling factor becomes inactive at low temperatures because of disappearance the influence of the inner ring for creating the small oscillations.

3.3. XOR gate

The magnetic flux plays an important role in electron transport and is fundamental to designing nanoscale XOR gate by tuning gate voltage applied to the outer ring. The transmission probability as a function of injecting electron energy was studied for CDQR. Two gate voltages (V_{g1} and V_{g2}) were treated as the two inputs of the XOR gate. The results in Fig. 8(a) show the XOR gate action, where the transmission probability was plotted at magnetic flux Φ=Φ◦/2. There are two cases of transmission probability describe the XOR gate action. One case, the transmission probability is died out when the two gate voltages were symmetric (V_{g1}=V_{g2}=0) or (V_{g1}=V_{g2}=0.4V) due to the symmetry between eigenvalues of atomic sites in the upper and the lower arm of the outer ring. This the symmetry between eigenvalues of atomic sites leads to destructive interference. Another case, the non-vanishing behavior of the transmission probability when the two gate voltages were asymmetric, in other words, one of two gate voltages is high and other is low. This fact can be understood as follows, because broken of symmetries between the eigenvalues of atomic sites found in upper and lower arm of the outer ring. The asymmetry between upper and lower arms of outer ring leads to constructive interference. The destructive and constructive interference are controlled by probability amplitude of electron passing through the outer ring $|\varphi_1 + \varphi_2|^2 = 2\varphi_0^2[1 + cos(2\pi\Phi/\Phi_0)]$. Where φ_1 and φ_2 are the electronic wave functions of electron passing through upper and lower arms, respectively [30]. All the resonant peaks were associated with the energy eigenvalues of the CDQR, and therefore, it can be claimed that the transmission probability determines the electronic structure of the CDQR.

To visualize the XOR gate action more noticeably, the variety of current (in a unit of $2e/h$) as a function of bias voltage was presented in Fig. 8(b). Here the temperature is fixed at 300 K. The chemical potentials for two leads can be adjusted by using a bias voltage. Since transmission probability through CDQR vanished completely for the entire energy range when both the two inputs of gate voltage were low (V_{g1}=V_{g2}=0) or high (V_{g1}=V_{g2}=0.4). As the result, the electric current vanishes in this case. While the current reveals step-like behavior when anyone of gate voltages is low and other is high. The current increases by increasing the bias voltage, where reached to 0.95 ($2e/h$) at bias voltage V_{bias}=3V, because of rising the difference between the chemical potentials of the two leads. Subsequently, the number of energy levels within the effective region will increase, this fact will lead to increase the number of electrons passing through the CDQR.

4. Conclusion

To summarize, the electron transport through the outer ring of a concentric double quantum ring device was examined in dependence on magnetic flux, which threaded both rings. Some resonant peaks of transmission probability were degenerating under the effect of magnetic flux at fixed value of inter-ring tunnel coupling. But, most resonant peaks and antiresonance disappear when the AB phase $\phi = 2\pi$ for several values of inter-ring coupling, except the one antiresonance localized about=1Γ. The two types of oscillations observed in conductance spectrum, one called normal AB oscillations and other is small oscillations above AB oscillations due to the influence of inner ring on electron transport in the outer ring. The strengthening of inter-ring tunnel coupling (t) led to a non-monotonic variation of the small oscillations at symmetric values of gate voltage. While the increasing of inter-ring tunnel coupling led to monotonically enhancement of the small oscillations at asymmetric values of gate voltage. In addition to that, the influence of Coulomb interaction and the number of electrons on small oscillations is investigated. The Coulomb interaction led to increasing the electrical conductance, while ratio the number of electron to the number of sites determined the periodicity of small oscillations. The influence of the inner ring for construction the small oscillations became inactive at low temperature. We consider that the influence of both magnetic flux and gate voltage on the electron transport properties offered attractive new strategies to nanoscale logic gates based on quantum rings. Finally, the nanoscale XOR gate-like is designed by utilizing the magnetic flux independent electron transport and tuning gate voltages externally applied to the outer ring. The high (low) transmission and current occurred when both gate voltages were symmetric (asymmetric). These theoretical results will be useful to design nanoscale logical gates based on concentric double quantum ring molecular electronic devices and circuits with specific properties.

References

[1] M. Hasan, I.V. Iorsh, O.V. Kibis, I.A. Shelykh, Phys. Rev. B 93 (2016) 125401.
[2] Js Ferrando-Soria, E.M. Pineda, A. Chiesa, A. Fernandez, S.A. Magee, S. Carretta, P. Santini, Ii.J. Vitorica-Yrezabal, F. Tuna, G.A. Timco, Nat. Commun. 7 (2016).
[3] D. Cricchio, E. Fiordilino, Nanoscale 8 (2016) 1968–1974.
[4] M. Sam, K. Navi, M.H. Moaiyeri, Quantum Matter 5 (2016) 99–102.
[5] A. Shokri, S.M. Mirzanian, J. Mol. Model. 21 (2015) 1–7.
[6] S.M. Mirzanian, A.A. Shokri, J. Phys. Chem. Solids 77 (2015) 146–150.
[7] V.M. Fomin, Physics of Quantum Rings, NanoScience and Technology Springer, 2013.
[8] R.A. Webb, S. Washburn, C.P. Umbach, R.B. Laibowitz, Phys. Rev. Lett. 54 (1985) 2696.
[9] A. Mühle, W. Wegscheider, R.J. Haug, Physica E: Low.-Dimens. Syst. Nanostruct. 40 (2008) 1246–1248.
[10] T. Mano, T. Kuroda, S. Sanguinetti, T. Ochiai, T. Tateno, J. Kim, T. Noda, M. Kawabe, K. Sakoda, G. Kido, Nano Lett. 5 (2005) 425–428.

[11] I. Filikhin, S. Matinyan, J. Nimmo, B. Vlahovic, Physica E: Low.-Dimens. Syst. Nanostruct. 43 (2011) 1669–1676.
[12] J.I. Climente, J. Planelles, M. Barranco, F. Malet, M. Pi, Phys. Rev. B 73 (2006) 235327.
[13] J.M. Escartín, F. Malet, M. Barranco, M. Pi, Physica E: Low.-Dimens. Syst. Nanostruct. 42 (2010) 841–843.
[14] H.M. Baghramyan, M.G. Barseghyan, D. Laroze, A.A. Kirakosyan, Physica E: Low.-Dimens. Syst. Nanostruct. 77 (2016) 81–89.
[15] M.R. Fulla, J.H. Marín, D. Londoño, C.A. Duque, M.E. Mora-Ramos, Acta Physica Pol. A 125 (2014) 220–223.
[16] H.K. Salehani, M. Esmaeilzadeh, K. Shakouri, M.R. Abolhassani, E. Faizabadi, M.H. Majlesara, Int. J. Nanosci. Nanotechnol. 7 (2011) 65–71.
[17] A. Mühle, W. Wegscheider, R.J. Haug, Appl. Phys. Lett. 91 (2007) 133116.
[18] J.W. Silverstone, R. Santagati, D. Bonneau, M.J. Strain, M. Sorel, J.L. O'Brien, M.G. Thompson, Nat. Commun. 6 (2015).
[19] A. Kregar, J.H. Jefferson, A. Ramšak, Phys. Rev. B 93 (2016) 075432.
[20] L.F. Al-Badry, Recent Patents on Nanotechnology, 10.
[21] S.K. Maiti, Solid State Commun. 149 (2009) 2146–2150.
[22] S.K. Maiti, Phys. Lett. A 373 (2009) 4470–4474.
[23] H. Khanzadi, H.K. Salehani, J. Nanosci. Technol. 2 (2016) 119–121.
[24] L.F. Al-Badry, Physica E: Low.-Dimens. Syst. Nanostruct. 83 (2016) 201–206.
[25] S. Datta, Quantum Transport: Atom to Transistor, Cambridge University Press, Cambridge, 2005.
[26] G.-Y. Chen, Y.-N. Chen, D.-S. Chuu, Solid State Commun. 143 (2007) 515–518.
[27] C.J. Lambert, Chem. Soc. Rev. 44 (2015) 875–888.
[28] F.V. Kusmartsev, J. Phys.: Condens. Matter 3 (1991) 3199.
[29] F.V. Kusmartsev, J.F. Weisz, R. Kishore, M. Takahashi, Phys. Rev. B 49 (1994) 16234.
[30] L.F. Al-Badry, Recent Pat. Nanotechnol. 11 (2017) 63–69.